Enhancement of electromagnetically induced absorption with elliptically polarized light - laser intensity dependent coherence effect

J. Dimitrijević, Z. Grujić, M. Mijailović, D. Arsenović, B. Panić and B. M. Jelenković

Institute of Physics, Pregrevica 118, Belgrade, Serbia

jelenad@phy.bg.ac.yu

Abstract: Using the $^2S_{1/2}F_g = 2 \longrightarrow {}^2P_{3/2}F_e = 3$ transition in ^{87}Rb vapor at room temperature, we study effect of the laser light polarization on the electromagnetically induced absorption (EIA). This work extends the recent study of the behavior of the EIA as a function of the laser ellipticity (Brazhnikov et. al., JETP Lett. 83, 64, 2006). We have shown that such behavior strongly depends on the laser power. For the low laser power EIA amplitude has maximum for linearly polarized light, while for high laser power elliptically polarized light of ellipticity $15-20^\circ$ generates maximum of the EIA amplitude. EIA width varies slowly with the laser ellipticity at lower laser power, and much stronger at higher laser power. Through our theoretical model we attributed observed results to combined effect of the laser ellipticity and power on the population of ground state Zeeman sublevels.

OCIS codes: (270.1670) Coherent optical effects, (300.1030) Absorption

References and links

1. E. Arimondo, “Coherent population trapping in laser spectroscopy,” Prog. Opt. **35**, 257-354 (1996).
2. A. M. Akulshin, S. Barreiro, and A. Lezama, “Electromagnetically induced absorption and transparency due to resonant two-field excitation of quasidegenerate levels in Rb vapor,” Phys. Rev. A **57**, 2996-3002 (1998).
3. A. V. Taichenachev, A. M. Tumaikin, and V. I. Yudin, “Electromagnetically induced absorption in a four-state system,” Phys. Rev. A **61**, 011802(R)-4, (1999).
4. C. Goren, A. D. Wilson-Gordon, M. Rosenbluh, and H.Friedmann, “Electromagnetically induced absorption due to transfer of coherence and to transfer of population,” Phys. Rev. A **67**, 033807-8 (2003).
5. P. Marte, P. Zoller, and J. L. Hall, “Coherent atomic mirrors and beam splitters by adiabatic passage in multilevel systems,” Phys. Rev. A **44**, R4118-R4121 (1991).
6. L. S. Goldner, C. Gerz, R. J. C. Spreeuw,S. L. Rolston, C. I. Westbrook, W. D. Phillips, P. Marte, and P.Zoller, “Momentum transfer in laser-cooled cesium by adiabatic passage in a light field,” Phys. Rev. Lett. **72**, 997-1000 (1994).
7. M. Weitz, T. Heupel, T. W. Hansch, “Collapse and revival of the fringe pattern in a multiple-beam atom interferometer,” Europhys. Lett. **37**, 517-522 (1997).
8. A. B. Matsko, I. Novikova, M. S. Zubairy and G. R. Weltch, “Nonlinear magneto-optical rotation of elliptically polarized light,” Phys. Rev. A **67**, 043805-18 (2003).
9. A. V. Taichenachev, A. M. Tumaikin, V. I. Yudin, “Invariant treatment of coherent population trapping in an elliptically polarized field,” Europhys. Lett. **45**, 301-306 (1999).
10. A. V. Taichenachev, V. I. Yudin, V. L. Velichansky, A. S. Zibrov, and S. A. Zibrov, “Pure superposition states of atoms generated by a bichromatic elliptically polarized field,” Phys. Rev. A **73**, 013812-5 (2006).

#90505 - $15.00 USD Received 4 Dec 2007; revised 11 Jan 2008; accepted 11 Jan 2008; published 17 Jan 2008

11. S. A. Zibrov, V. L. Velichansky, A. S. Zibrov, A. V. Taichenachev, and V. I. Yudin, "Experimental preparation of pure superposition states of atoms via elliptically polarized bichromatic radiations," Opt. Lett. **31**, 2060-2062 (2006).
12. F. Renzoni, C. Zimmermann, P. Verkerk, and E. Arimondo, "Enhanced absorption Hanle effect on the Fg=F - Fe=F+1 closed transitions," J. Opt. B: Quantum Semiclass. Opt. **3**, S7-S14 (2001).
13. A. V. Taichenachev, A. M. Tumaikin, V. I. Yudin, and G. Nienhuis, "Steady state of atoms in a resonant field with elliptical polarization," Phys. Rev. A **69**, 033410-18 (2004).
14. D. V. Brazhnikov, A. M. Tumaikin, V. I. Yudin, and A. V. Taichenachev, "Electromagnetically induced absorption and transparency in magneto-optical resonances in an elliptically polarized field," J. Opt. Soc. Am. B **22**, 57-64 (2005).
15. D. V. Brazhnikov, A. V. Taichenachev, A. M. Tumaikin, V. I. Yudin, S. A. Zibrov, Y. O. Dudin, V. V. Vasilev, V. L. Velichansky, "Features of magneto-optical resonances in an elliptically polarized traweling light wave," JETP Lett. **83**, 64-68 (2006).
16. S. D. Badger, I. G. Hughes and C. S. Adams, "Hyperfine effects in electromagnetically induced transparency," J. Phys. B **34**, L749-L756 (2001).
17. A. K. Patnaik, P. S. Hsu, G. S. Agarwal, G. R.Welch, and M. O. Scully, "Measurement of ground-state decoherence via interruption of coherent population trapping," Phys. Rev. A **75**, 023807-6 (2007).
18. A. Huss, R. Lammegger, L. Windholz, E. Alipieva, S. Gateva, L. Petrov, E. Taskova, and G. Todorov, "Polarization-dependent sensitivity of level-crossing, coherent-population-trapping resonances to stray magnetic fields," J. Opt. Soc. Am. B **23**, 1729-1736 (2006).
19. J. Dimitrijević, A. Krmpot, M. Mijailović, D. Arsenović, B. Panić, Z. Grujić andB. M. Jelenković, "Role of transverse magnetic fields in electromagnetically induced absorption for elliptically polarized light," Phys Rev A (to be published).
20. J. Dimitrijević, D. Arsenović, and B. M. Jelenković, "Intensity dependence narrowing of electromagnetically induced absorption in a Doppler-broadened medium," Phys. Rev. A **76**, 013836-7 (2007).

1. Introduction

Coherent interaction of atoms with electromagnetic fields can lead to optical pumping into coherent superposition (of either hyperfine or magnetic sublevels) which, in some cases is non-coupled, and in other cases very strongly coupled, with the original electromagnetic fields. In the former case coherent population trapping (CPT) and electromagnetically induced transmission (EIT) or "dark" state is generated [1]. In the latter case medium posses properties named electromagnetically induced absorption (EIA) [2]. Both types of coherent interactions have attracted great attention due to many interesting applications.

In this work we study effects of the laser ellipticity on the properties of sub-Doppler EIA resonances. As explained in [2], EIA can be observed in a two level atom if the degeneracy of excited state is greater then the degeneracy of the ground state by one. Closed transitions in alkali atoms $F_g \rightarrow F_e = F_g + 1$, where $F_{g,e}$ are atomic angular momentum for the ground and excited states, have been used to generate EIA. EIA is explained as spontaneous transfer of the anisotropy induced in an excited state (atomic coherence or/and population difference) to the ground state levels of an atom [3, 4]. EIA media is very much different from EIT media, not only because of the different sign of the transmission resonance. Non-linear magneto-optical polarization rotation has opposite sign in EIA and EIT medium. Group velocity of the light tuned to EIT transition can be much smaller then the speed of light because of normal dispersion near the EIT resonance, while abnormal dispersion near the EIA resonance leads to "fast" or subluminal light.

Of the two phenomena, EIT was studied more intensely then EIA, and most of investigations of both EIT and EIA were with linearly polarized light. This is despite importance of elliptically polarized light for adiabatic momentum transfer [5, 6], and multi-path atomic interferometry [7]. For EIT, propagation of strong elliptically polarized light through resonant atomic medium in the presence of external magnetic field, for different Λ and M systems, was investigated, both experimentally and theoretically [8]. CPT under the interaction of elliptically polarized light, was analytically treated in [9]. Recently, it was shown that elliptically polarized light is necessary for the preparation of CPT which is due to pure superposition of magnetic sublevels

#90505 - $15.00 USD Received 4 Dec 2007; revised 11 Jan 2008; accepted 11 Jan 2008; published 17 Jan 2008

(belonging to two ground state hyperfine levels) with the same m number ($m-m$ states) [10, 11]. Numerical calculations of the total excited state populations for closed transitions in Rb were done for linearly and for circularly polarized light [12]. Theoretical study of interactions of resonant radiation fields with arbitrarily polarization, for transitions with arbitrary relation between angular momentum of the ground and excited states (including transition $J_g \rightarrow J_e = J_g + 1$, was thoroughly done by Taichenachev et al. [13]. Effect of ellipticity of the laser light on Hanle EIA was presented in [14] by an analytical solution of the model for $F_g = 1 \rightarrow F_e = 2$ atomic transition. They show Doppler narrowing of the EIA widths for elliptically polarized light, and EIA narrowing with increased light ellipticity for the same Doppler width. More recently, the same group have shown dependence of EIA amplitude and width on the light polarization for $F_g = 2 \rightarrow F_e = 3$ transition in ^{87}Rb [15]. They showed, for given laser power of 3 mW, that the EIA amplitude increases with the laser ellipticity, and has maximum value for high laser light ellipticity. This is different behavior than behavior of CPT as a function of the laser ellipticity. It was shown that absorption of light that interacts with Λ atomic scheme does not depend so strongly on the ellipticity of the light [8].

In this work we made theoretical and experimental investigations of the EIA resonance line shape, amplitude and width using laser light of different ellipticity and different intensities. Experimentally, we measured Hanle EIA profiles, i.e, transmission of the laser beam through the Rb vapor in the presence of variable magnetic field, directed orthogonal to the polarization ellipse. Theoretically, we calculated laser absorption from diagonal elements of a density matrix, calculated after solving optical Bloch equations for the atomic system investigated experimentally. Final theoretical results were obtained after averaging over Doppler broadening.

2. Theoretical model

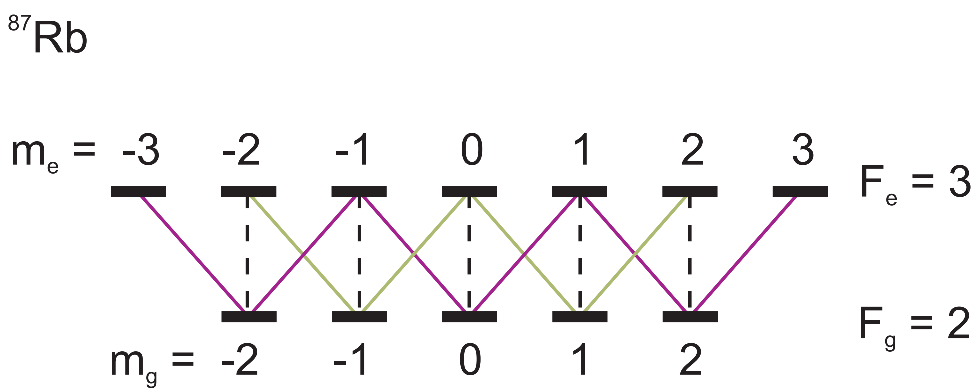

Fig. 1. Level diagram for the $F_g = 2 \rightarrow F_e = 3$ transition of ^{87}Rb. Full lines stand for transitions induced by elliptically polarized laser light, while both full and dashed lines describe spontaneous emission.

In this section we present model used to calculate Hanle EIA, i.e., the transmission of a laser beam, resonant to the closed $F_g = 2 \rightarrow F_e = 3$ transition in ^{87}Rb (see Fig. 1), as a function of external magnetic field B_{scan}. Comparison of the model with the experiment is done by solving Optical Bloch equations for the atomic system given schematically in Fig. 1. The density matrix is denoted by ρ, where $\rho_{g_i g_j}$ and $\rho_{e_i e_j}$ are elements of density submatrices for the ground and excited state. The elements $\rho_{e_i g_j}$ and $\rho_{g_i e_j}$ describe the optical coherences, and in rotating wave

#90505 - $15.00 USD Received 4 Dec 2007; revised 11 Jan 2008; accepted 11 Jan 2008; published 17 Jan 2008

approximation the substitution

$$\rho_{e_i g_j} = \tilde{\rho}_{e_i g_j} e^{-i\omega t} \tag{1}$$

is introduced.

Properties of light enter the equations through the electric field vector $\vec{E}$ and it runs along z-axis, which is also the direction of $\vec{B}_{scan}$. For a laser light of arbitrary ellipticity ε (defined by $\tan\varepsilon = \frac{E_{0y}}{E_{0x}}$) it holds:

$$\vec{E}(t) = \vec{e}_x \cos(\omega t) E_{0x} + \vec{e}_y \cos(\omega t + \varphi^{yx}) E_{0y}. \tag{2}$$

Here, ω is the laser frequency, E_{0x} and E_{0y} are amplitudes of major and minor polarization's ellipse semi-axes. φ^{yx} is the phase difference between these two components and we take it always to be $+\pi/2$ meaning that electric vector traces out an ellipse with axes along x and y axes and rotates clockwise as it propagates along z-axis.

Energies describing the Zeeman splitting of the ground and the excited levels with magnetic quantum numbers $m_{g(e)}$, $E_{g(e)} = \omega_{g(e)}\hbar$, due to applied magnetic field B_{scan}, were calculated using

$$E_{g(e)} = \mu_B g_{F_{g(e)}} m_{g(e)} B_{scan}. \tag{3}$$

Here μ_B is the Bohr magneton and $g_{F_{g(e)}}$ is the Lande gyromagnetic factor for two hyperfine levels ($1/2$ for the ground and $2/3$ for the excited state).

Dipole moment matrix elements are given by:

$$\mu_{m_e,m_g,q} = e\langle m_e|\vec{u}_q\vec{r}|b\rangle = \mathscr{G}_1(-1)^{-m_e}\begin{pmatrix} 2 & 1 & 3 \\ m_g & q & -m_e \end{pmatrix} \tag{4}$$

with the spherical orths $\vec{u}_{-1} = \frac{\vec{e}_x - i\vec{e}_y}{\sqrt{2}}$, $\vec{u}_{+1} = -\frac{\vec{e}_x + i\vec{e}_y}{\sqrt{2}}$ and $\vec{u}_0 = \vec{e}_z$. $\mathscr{G}_1$ is the constant proportional to the reduced matrix element of the dipole operator between the ground and the excited states

$$\mathscr{G}_1 \sim \langle n_e L_e \|\vec{r}\| n_g L_g\rangle. \tag{5}$$

The value of the reduced matrix element is taken from [16]. The quantities

$$\mathscr{G}_{2i} = \frac{E_{0i}}{2\sqrt{2}\hbar}, i = x, y \tag{6}$$

are also introduced.

The optical Bloch equations for the closed system, and including the ground state relaxation, have the form:

$$\begin{aligned}
\dot{\rho}_{e_i e_j} &= [-\frac{2}{7}\Gamma_L|\mathscr{G}_1|^2 + i(\omega_{e_j} - \omega_{e_i})]\rho_{e_i e_j} + \\
& i\sum_{l=-2}^{2}[\tilde{\rho}_{e_i g_l}(\mu_{g_l,e_j,-1}(-\mathscr{G}_{2x} - ie^{i\varphi^{yx}}\mathscr{G}_{2y}) + \mu_{g_l,e_j,1}(\mathscr{G}_{2x} - ie^{i\varphi^{yx}}\mathscr{G}_{2y})) + \\
& (\mu_{e_i,g_l,-1}(\mathscr{G}_{2x} + ie^{-i\varphi^{yx}}\mathscr{G}_{2y}) + \mu_{e_i,g_l,1}(-\mathscr{G}_{2x} + ie^{-i\varphi^{yx}}\mathscr{G}_{2y}))\tilde{\rho}_{g_l e_j}] - \gamma\rho_{e_i e_j} \\
\dot{\tilde{\rho}}_{e_i g_j} &= [-\frac{\Gamma_L}{7}|\mathscr{G}_1|^2 + i(\omega + \omega_{g_j} - \omega_{e_i})]\tilde{\rho}_{e_i g_j} + \\
& i\{\sum_{l=-3}^{3}[\rho_{e_i e_l}(\mu_{e_l,g_j,-1}(-\mathscr{G}_{2x} - ie^{-i\varphi^{yx}}\mathscr{G}_{2y}) + \mu_{e_l,g_j,1}(\mathscr{G}_{2x} - ie^{-i\varphi^{yx}}\mathscr{G}_{2y}))] + \\
& \sum_{l=-2}^{2}[(\mu_{e_i,g_l,-1}(\mathscr{G}_{2x} + ie^{-i\varphi^{yx}}\mathscr{G}_{2y}) + \mu_{e_i,g_l,1}(-\mathscr{G}_{2x} + ie^{-i\varphi^{yx}}\mathscr{G}_{2y}))\rho_{g_l g_j}]\} - \gamma\tilde{\rho}_{e_i g_j}
\end{aligned}$$

#90505 - $15.00 USD Received 4 Dec 2007; revised 11 Jan 2008; accepted 11 Jan 2008; published 17 Jan 2008

$$
\begin{aligned}
\dot{\tilde{\rho}}_{g_j e_i} &= [-\frac{\Gamma_L}{7}|\mathscr{G}_1|^2 + i(-\omega + \omega_{e_i} - \omega_{g_j})]\tilde{\rho}_{g_j e_i} + \\
& i\{\sum_{l=-2}^{2}[\rho_{g_j g_l}(\mu_{g_l,e_i,-1}(-\mathscr{G}_{2x} - ie^{i\varphi^{yx}}\mathscr{G}_{2y}) + \mu_{g_l,e_i,1}(\mathscr{G}_{2x} - ie^{i\varphi^{yx}}\mathscr{G}_{2y})] + \\
& \sum_{l=-3}^{3}[(\mu_{g_j,e_l,-1}(\mathscr{G}_{2x} + ie^{i\varphi^{yx}}\mathscr{G}_{2y}) + \mu_{g_j,e_l,1}(-\mathscr{G}_{2x} + ie^{i\varphi^{yx}}\mathscr{G}_{2y}))\rho_{e_l e_i}]\} - \gamma\tilde{\rho}_{g_j e_i} \\
\dot{\rho}_{g_i g_j} &= [2\sum_{q=-1}^{1}\mu_{e_{i+q},g_i,q}\mu^*_{e_{j+q},g_j,q}\rho_{e_{i+q}e_{j+q}}\Gamma_L + i(\omega_{g_j} - \omega_{g_i})\rho_{g_i g_j}] + \\
& i\sum_{l=-3}^{3}[\tilde{\rho}_{g_i e_l}(\mu_{e_l,g_j,-1}(-\mathscr{G}_{2x} - ie^{-i\varphi^{yx}}\mathscr{G}_{2y}) + \mu_{e_l,g_j,1}(\mathscr{G}_{2x} - ie^{-i\varphi^{yx}}\mathscr{G}_{2y})) + \\
& (\mu_{g_i,e_l,-1}(\mathscr{G}_{2x} + ie^{i\varphi^{yx}}\mathscr{G}_{2y}) + \mu_{g_i,e_l,1}(-\mathscr{G}_{2x} + ie^{i\varphi^{yx}}\mathscr{G}_{2y}))\tilde{\rho}_{e_l g_j}] - \gamma(\rho_{g_i g_j} - \frac{1}{5}\delta_{ij}).
\end{aligned} \tag{7}
$$

In Eq. 7, real part of first term of right-hand side comes from spontaneous emission. We take $\frac{2}{7}\Gamma_L|\mathscr{G}_1|^2 = \Gamma$, where $\Gamma = 2\pi \cdot 6.07\,\mathrm{MHz}$ is total spontaneous emission rate of any excited sublevel. Imaginary part in Eq. 7 describes free evolution of matrix elements $\rho_{g_i g_j}$ and $\rho_{e_i e_j}$, while for $\rho_{e_i g_j}$ and $\rho_{g_i e_j}$ it stands for the detuning (difference between laser and resonance frequency) $\Delta_{Dji} = \omega - (\omega_{e_0} - \omega_{g_0})$. Second term comes from interaction of the laser light with atoms. The last term in the right hand-side of Bloch equation describes the ground state decoherence rate γ at which atoms enter and leave the laser beam. In the vacuum Rb cell at room temperature vapor pressure is about 3 x $10^{-}5$ Pa and therefore the role of atomic collisions on the coherence decay and resonance width can be neglected. The decay rate of the Zeeman ground sublevels coherence, transferred from the excited state via spontaneous emission, is effectively life time determined by the atom transit time through the laser beam. Most of presented results were calculated for γ determined from the atom transit time through laser beam [17]. The atoms fly in the laser beam long enough so they reach steady state: they recycle between ground and excited state hundreds of times during the transit time through the laser beam. Therefore, we set time derivations in left-hand side of Bloch equations to zero and then solve them as linear algebraic equations. As a spectroscopic signal we consider the total excited-state population

$$
\Pi_e = \sum \rho_{e_i e_i}. \tag{8}
$$

as a function of the magnetic field amplitude B_{scan}. This number is proportional to fluorescence signal. Since all atoms in the excited state decay at the same rate, this number is also proportional to the light absorption coefficient in optically thin media. As a laser transmission spectroscopic signal, we presented ground state population i.e., $(1 - \Pi_e)$. Simultaneous measurements of fluorescence and of laser transmission [18] show that both give same results for widths and amplitudes (up to constant). Since all of our results present ellipticity (not intensity) dependence, above subtraction doesn't change the mutual ratio of EIA amplitudes when compared for different ellipticities. The Doppler effect was taken into account by assuming Maxwell-Boltzmann velocity distribution for atoms at room temperature (300 K). We averaged contributions of atoms whose projections of velocities along laser light are in the interval $(-700, 700)\,\mathrm{m/s}$.

3. Experimental setup

The experimental setup used for measurements of the EIA in Hanle configuration is shown in Fig. 2. We use ECDL (External Cavity Diode Laser) which is frequency stabilized by DDAVLL

#90505 - $15.00 USD Received 4 Dec 2007; revised 11 Jan 2008; accepted 11 Jan 2008; published 17 Jan 2008

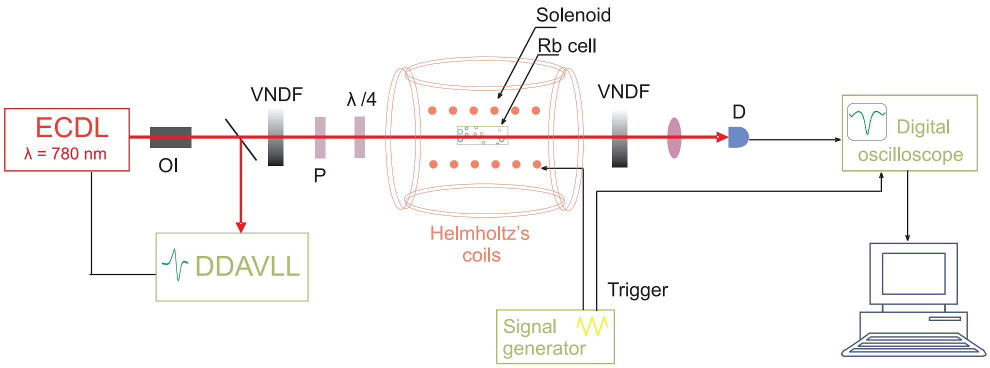

Fig. 2. Experimental setup: ECDL - external cavity diode laser; OI - optical isolator; DDAVLL - Doppler-free dichroic atomic vapor laser lock; VNDF - variable neutral density filter; P - polarizer; D - detector.

(Doppler free Dichroic Atomic Laser Lock) method at $F_g = 2 \rightarrow F_e = 3$ transition of ^{87}Rb (D2 line). The Faraday optical isolator (OI) prevents undesired feedback to the laser diode. Laser diameter is equal to 4.1 mm and was determined using the standard method of measurements of the Gaussian laser beam profiles. The Rb vapor cell used in experiment is 8 cm long and is located inside the long coil which produces variable magnetic field in the same direction as the laser beam propagation. The cell is placed at the center of three, large orthogonal pairs of Helmholtz's coils, in order to compensate laboratory magnetic field. Measured magnetic field inhomogeneity from one end of the Rb cell to the other was less then 1 mG. Recent estimation of effects of transverse (orthogonal to $\vec{B}_{scan}$) magnetic fields on amplitudes and widths of Hanle EIA show that stray magnetic fields of the order of a few mG can be neglected [19]. Variable neutral density filter (VNDF) is used to achieve desired laser intensity. Laser field ellipticity is controlled by the linear polarizer and $\lambda/4$ plate. The intensity of transmitted laser light is detected with photodiode (D) and recorded by the digital oscilloscope, while simultaneously recording voltage proportional to the current through the solenoid used for generating longitudinal magnetic field.

4. Results and discussion

Theoretical and experimental results of the EIA amplitudes and widths, which will be shown in the following figures, were derived from Hanle profiles. That is, from calculated and measured transmission of the laser power as a function of the external magnetic field (Hanle-type spectroscopy). EIA amplitudes were evaluated like the difference between transmission minimum at $B_{scan} = 0$ and value of the fit of Hanle profile, in the absence of EIA, also at $B_{scan} = 0$. Figure 3 shows dependence of the EIA amplitude as a function of the laser ellipticity for several laser powers. It is apparent that the EIA dependence on the laser ellipticity is influenced by the laser power. At low laser power, 50 μW, light of small ellipticity (theory) and linearly polarized light (experiment) is the most efficient in generating the EIA. At higher laser power, light of higher ellipticity is more efficient. As the laser power increases, so does the laser ellipticity at which the highest amplitude of the EIA is obtained. This shift of the EIA maximum towards higher laser ellipticity, as the laser power increases, occurs until laser powers reaches ~ 1 mW. At these laser powers we have exceeded saturation intensity for Rb. Light with ellipticity $\varepsilon = 15-20^\circ$ then gives maximum of the EIA.

Theoretical and experimental EIA amplitudes, given in Figs. 3(a) and 3(b) respectively, show very similar dependence on the laser ellipticity, for quoted laser powers. The differences is the

#90505 - $15.00 USD Received 4 Dec 2007; revised 11 Jan 2008; accepted 11 Jan 2008; published 17 Jan 2008

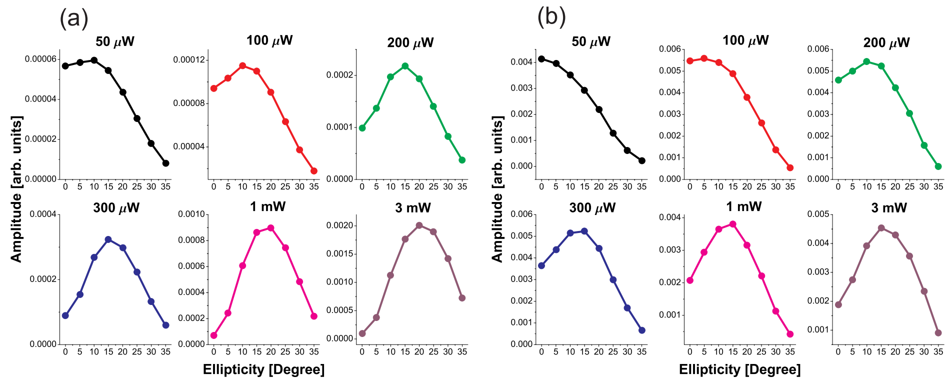

Fig. 3. Theoretical (a) and experimental (b) Hanle EIA amplitudes as a function of the laser light ellipticity for the laser powers between 50 μW and 3 mW.

value of the laser power at which linearly polarized light shows maximum of the EIA. Calculated results for lower laser power $\leq$20 μW (not shown) have the same behavior as a function of the laser ellipticity as experimental results at 50 μW - maximum of the EIA amplitude is for linearly polarized light. Note that our theoretical model did not take into account absorption of laser radiation as light propagates through Rb vapor and also Gaussian profile of the laser beam. Values for experimental and theoretical laser powers correspond to the input laser powers, before the Rb cell. Therefore, experimental results given in Fig. 3 correspond to averaged laser powers lower then the quoted powers for each graph. Also, maximum of the EIA given by the experiment is closer to the laser ellipticity of $\varepsilon = 15^\circ$, while theoretical maximum is closer to $\varepsilon = 20^\circ$. Such discrepancy can be due to uncertainties in determination of the laser ellipticity in the experiment. Experiment in [15], performed at 3 mW of the laser power (for the laser beam diameter of 5 mm), shows theoretically predicted dependence of the EIA amplitude on the laser ellipticity and maximum at the $\varepsilon = 20^\circ$.

It follows from results presented above, that efficiency of the laser light to produce EIA depends on the laser ellipticity, and that this dependence is different at different laser intensities. We will argue below that this behavior is due to a combination of effects of the laser intensity and polarization on optical pumping of the ground state sublevels. To do so, we analyzed characteristics of populations of ground state sublevels. Calculated results of the distribution of the population of the ground state Zeeman sublevels as a function of the external magnetic field, for the laser power of 50 μW and 1 mW are given in Figs. 4(a) and 4(b), respectively. For both laser powers results for three laser ellipticities are given. The population of $m_g = \pm 2$ and $m_g = \pm 1$ are given by red and green lines. Solid lines are for the population of $m_g = +1, +2$, while dashed-dot lines are for $m_g = -1, -2$ sublevels. Blue lines are for $m_g = 0$ sublevel. With our choice of positive phase ($\varphi^{yx} = +\pi/2$) and with positive E_{0x} and E_{0y}, σ^+ component of light is stronger or equal than σ^-, and elliptical light populates more sublevels with positive sign of m_g, particularly the edge sublevel $m_g = +2$. Note here that altering the sign of phase makes σ^- component dominant and consequently pumps sublevels with negative m_g. Nevertheless, overall results for Hanle EIA are not changed. At the same time amplitudes of the narrow structures (observed around $B_{scan} = 0$), for the sublevels that differ only in sign, are very similar but opposite in sign.

Results of Fig. 5 show interesting behavior of total population of even vs. odd magnetic sublevels. In Fig. 5 purple curves show population of even ($m_g = \pm 2, 0$) and green of odd ($m_g = \pm 1$) sublevels. According to level diagram in Fig. 1 even ground state magnetic sub-

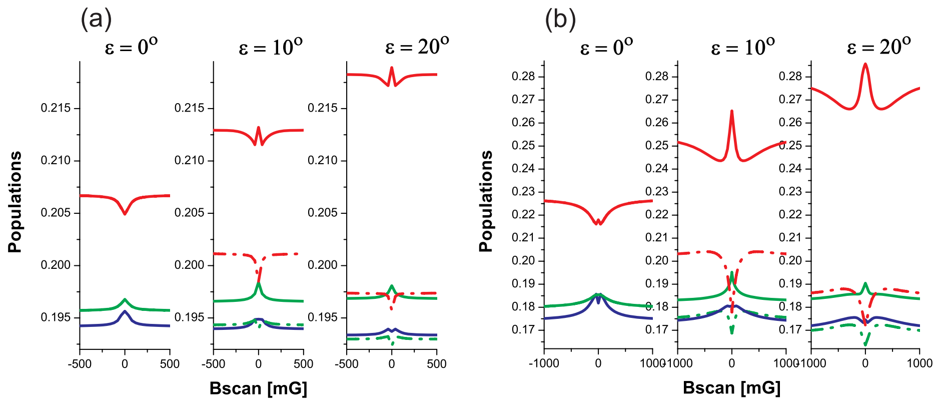

Fig. 4. Theoretical results for populations of ground states sublevels as a function of the external magnetic field, for three laser light ellipticities and for $P = 50\mu$W (a) and $P = 1$ mW (b); red and green lines are for populations of $m_g = \pm 2$ and $m_g = \pm 1$ sublevels, while blue lines are for $m_g = 0$ sublevel. Solid lines indicate populations of $m_g = +1, +2$, while dashed-dotted lines are for $m_g = -1, -2$ sublevels.

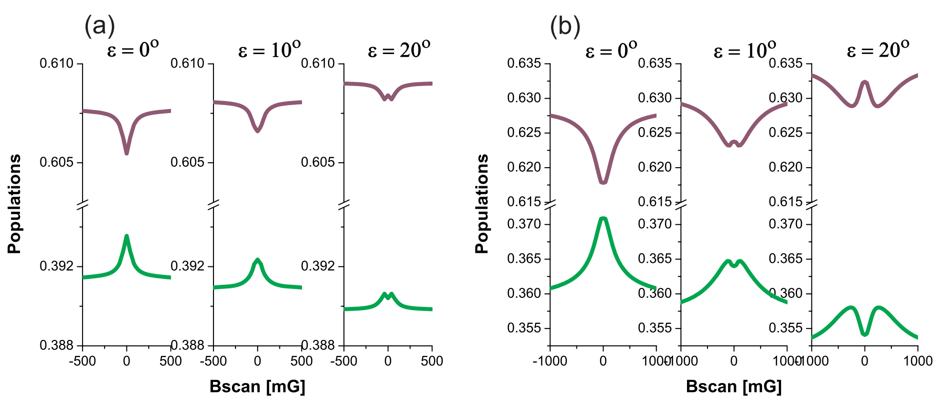

Fig. 5. Theoretical results for the sum of populations of ground state's sublevels as a function of the external magnetic field, for three laser light ellipticities and for $P = 50\mu$W (a) and $P = 1$ mW (b); purple lines: sum of populations of even m_gs; green lines: sum of populations of odd m_gs.

#90505 - $15.00 USD Received 4 Dec 2007; revised 11 Jan 2008; accepted 11 Jan 2008; published 17 Jan 2008

levels are part of one multiple V scheme, while odd ground state magnetic sublevels are part of different multiple V scheme. Nevertheless, division into odd and even sublevels reveals their population amplitudes are of opposite sign giving nearly a mirror image. It is never exactly the mirror image since the net result, Hanle EIA transmission curves, were always obtained. The comparison of the results for linear and elliptical light polarization (Figs. 5(a) and 5(b)) show intensity dependent splitting of the profile of the population curve for elliptically polarized light. However, such splitting in the population of magnetic sublevels showed no role in the overall Hanle profile of the transmitted laser light.

Results of Fig. 4 help towards understanding behavior of the complex EIA phenomena when both laser intensity and ellipticity varies. i.e., observed intensity dependence of the effect of ellipticity on the EIA amplitudes. Figs. 4(a) and 4(b) show that different Zeeman sublevels produce resonances with different sign (transmission/absorption gain), and that for the same magnetic sublevel the sign depends on the laser ellipticity. Optical pumping increases population of edged Zeeman sublevels, but even at high laser power imbalance of population among them is not so great to allow only edged sublevels to determine the shape of the resonance. Which sublevel contributes more to the EIA depends on both ellipticity and power. The narrower feature near $B_{scan} = 0$ gets almost completely cancelled in the total sublevel population and, for elliptical light and higher laser intensities transmission minimum of the total population (EIA) is mainly determined by the shape of the population of $m_g = +2$. The influence of edged sublevel on obtained result is increasing with the laser ellipticity and intensity. Results which we present here are characteristic of the Doppler broadened media. As we showed in [20] for linearly polarized laser light, dependence of EIA amplitude on the laser intensity also depends on atomic velocity. Figure 5 in [20] show that in Doppler broadened media EIA has a maximum at the laser intensity ~ 1.5 mW/cm^2. Figure 6, also in [20], show that, for an atom with defined velocity, the laser intensity at which EIA has a maximum, increases with the atom velocity. We don't present here results for EIA for a single atom velocity, but there is a big influence, as in [20], of the Doppler effect on the behavior of the EIA as the laser intensity and ellipticity change. It can be said that the EIA behavior at different laser power and ellipticity is a delicate balance between optical pumping, contributions of the population of different Zeeman sublevels and of atomic velocity. Elliptically polarized light pumps atoms in high Zeeman sublevels, strongly coupled by the same light to excited states, process which depends on the laser ellipticity, intensity and on atomic velocity.

Experimental and theoretical EIA widths are shown in Fig. 6(a) and 6(b). Results, given in units of B_{scan} (mG), are Full-Width Half-Maximum (FWHM) i.e., values of the scanning external magnetic field which splits the Zeeman sublevels and reduces the EIA amplitude at half of its value at zero scanning magnetic field. As seen in Fig. 6 width varies slowly with the laser ellipticity as long as the laser power is low. Theory and experiment show qualitatively the same behavior of EIA widths as a function of the laser ellipticity and power. Quantitative difference, higher values of EIA widths for calculated results, can be attributed to already mentioned difference between quoted and averaged power in the cell, i.e., to the fact that the experiment is performed at the average power lower that the power used in the calculations.

Our theoretical results were obtained from Hanle profiles using $\gamma = \frac{\Gamma}{529}$, where γ is the ground state decoherence rate. This value is determined from the atom transit time through the laser beam, using formula for averaged time of flight as in [17]. Considering this is an approximation, we looked into the dependence of the Hanle profiles for the different values of γ. Theoretical Hanle profiles for different laser ellipticity and for different values of γ and for two laser powers (50 μW and 1 mW) are presented in figure 7(a) and 7(b). For the comparison with the experiment we give experimental Hanle curves for the same laser power and ellipticity (top rows). As shown in Fig. 7 values of γ strongly influence profiles of the Hanle EIA, and consequently, γ has

#90505 - $15.00 USD Received 4 Dec 2007; revised 11 Jan 2008; accepted 11 Jan 2008; published 17 Jan 2008

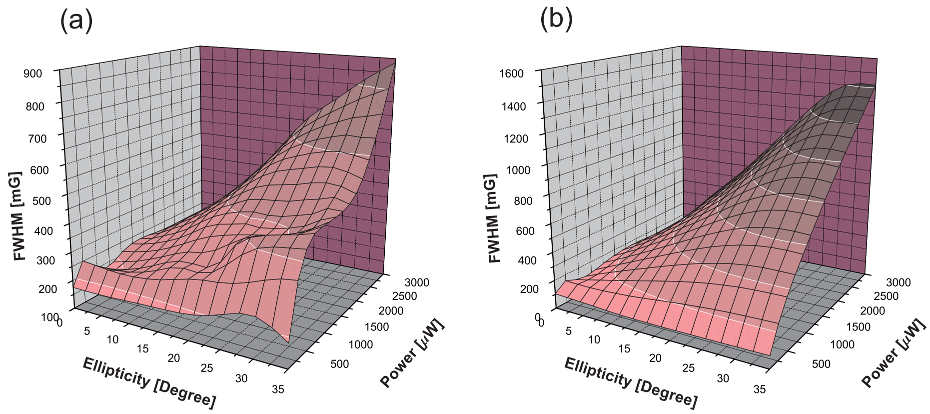

Fig. 6. 3D vision for Hanle EIA widths as a function of the laser light ellipticity and power: experimental (a), and calculated (b).

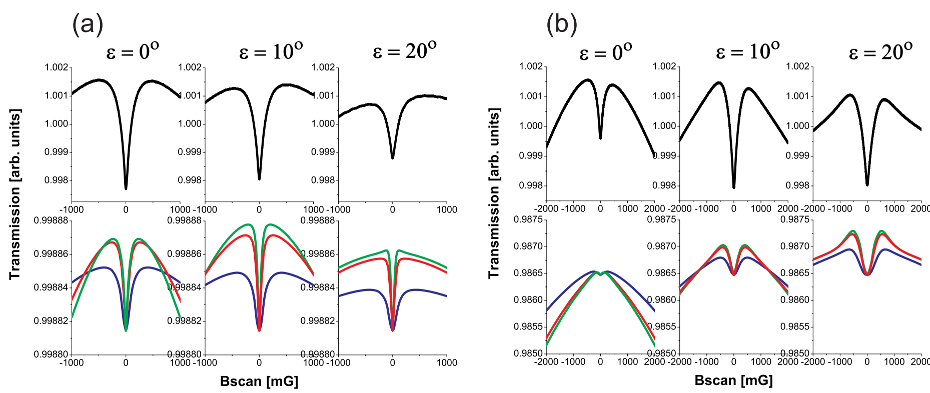

Fig. 7. Comparison of Hanle EIA spectra for the transition $F_g = 2 \rightarrow F_e = 3$ between experimental (top row) and calculated (bottom row) for two laser powers, 50 μW (a) and 1 mW (b). Theoretical results show influence of the ground state decoherence rate γ for three different values: blue lines: $\gamma = \frac{\Gamma}{100}$; red lines: $\gamma = \frac{\Gamma}{529}$; green lines: $\gamma = \frac{\Gamma}{1000}$. Theoretical curves for different γ were shifted along y-axis to have the same value for $B_{scan} = 0$.

a strong influence on the EIA amplitude and width. Increase of γ shifts maximum of the EIA amplitudes towards lower ellipticities for low laser power. Changing γ gives qualitatively similar behavior of EIA widths (which we present in units of B_{scan}) as in Fig. 6 (b). Quantitatively, results of Figs. 7 emphasize importance of γ in calculating EIA widths .

5. Conclusion

We have demonstrated theoretically and experimentally influence of the laser intensity on efficiency of generation of EIA with the laser light of specific ellipticity. We can also say that the results show different influence of the laser ellipticity on the EIA depending on the laser intensity. The two sentences emphasize the fact that observed EIA behavior is result of combined effect of the laser ellipticity and intensity. Our results show that maximum of the EIA occurs for linearly polarized light when the laser intensity is low, and that maximum of the EIA

#90505 - $15.00 USD Received 4 Dec 2007; revised 11 Jan 2008; accepted 11 Jan 2008; published 17 Jan 2008

amplitude moves towards higher laser ellipticity as the laser power increases. For higher laser intensity elliptically polarized light can enhance EIA amplitudes by a large factor in respect to linearly polarized light. We have also presented the behavior of EIA widths depending on both laser power and ellipticity. Calculated dependence of the population of Zeeman sublevels of the ground hyperfine level, and results with no Doppler effect (some relevant results were previously published [20]) helped to understand that observed behavior of the EIA at arbitrary laser ellipticity and power is not the result of an effect of a single parameter. Instead, EIA behavior at different laser power and ellipticity is due to (1) optical pumping into Zeeman sublevels, (2) contributions of different Zeeman sublevels to the total laser absorption even at high laser power, and (3) atomic velocity.

Acknowledgments

This work was supported by the Ministry of science of the Republic of Serbia, under grant number 141003.

#90505 - $15.00 USD Received 4 Dec 2007; revised 11 Jan 2008; accepted 11 Jan 2008; published 17 Jan 2008